


ORIGINAL PAPER

Open Access



Characterization the effects of nanofluids and heating on flow in a baffled vertical channel

Ali Assim Al-Obaidi^{1*}, Ali J. Salman¹, Ali Raheem Yousif¹, Dalya H. Al-Mamoori², Mohamed H. Mussa³, Tayser Sumer Gaaz², Abdul Amir H. Kadhum³, Mohd S. Takriff³ and Ahmed A. Al-Amieriy⁴ 

Abstract

The laminar 2-D blended convection of the nanofluids at different volume fractions has gained interest in the last decade due to an enormous application in technology. The laminar-flow stream system can be further modified by changing the geometry of the channel, adding an external heating source, and changing the initial conditions at which the stream is being influenced. The investigation of this system includes the variation of the geometrical parameters of the channel, Reynolds number, Nusselt number, and type of the nanoparticles used in preparing the nanofluid with water as the base fluid. These parameters constitute a very successful leading to utilize the numerical solutions by using a finite volume method. Regarding heat flow, one side of the channel was supplied by the heat while the temperature of the other side was kept steadily. The upstream walls of the regressive confronting step were considered as adiabatic surfaces. The nanofluids were made by adding aluminum oxide (Al_2O_3), copper oxide (CuO), silicon dioxide (SiO_2), or zinc oxide (ZnO) nanoparticles to various volume fractions in the scope of 1 to 4% and diverse nanoparticle diameters of 25 to 80 nm. The calculations were performed with heat flux, Reynolds numbers (Re), and step height (S) at a range of $100 < q < 600 \text{ W/m}^2$, $100 < Re < 500$, and $3 \leq S \leq 5.8$, respectively. The numerical study has shown that the nanofluid with SiO_2 has the highest value of the Nusselt number (Nu). The distribution area and the Nu increase as Reynolds number increases and diminish as the volume fraction diminishes with the increase of the nanoparticle diameter. The outcome of this paper has shown that assisting flow has shown superiority over the opposing flow when Nu increases.

Keywords: Blended convection, Backward-facing step, Channel flow, Nanofluids

Introduction

The regressive confronting step stream is a basic idea that provides a straightforward geometrical model of complex solutions for stream detachment and reattachment (D'Adamo, Sosa, & Artana, 2014). Some application examples include cooling turbine blades, chemical processes, cooling of nuclear reactors, wide angle diffusers, high-performance heat exchangers, energy system equipment, and flow in valves. Heat transfer in separated flows is frequently encountered in various engineering applications centrifugal compressor blades, gas turbine blades, and microelectronic circuit boards

(Hashim et al., 2018; Ma, Mohebbi, Rashidi, & Yang, 2018a, 2019; Mohebbi & Heidari, 2017; Mohebbi, Izadi, & Chamkha, 2017; Mohebbi, Izadi, Delouei, & Sajjadi, 2019; Mohebbi, Rashidi, Izadi, Sidik, & Xian, 2018; Ranjbar, Mohebbi, & Heidari, 2018). A thorough comprehensive detail of these streams constitutes a prime significance outlining constructing devices such as combustors, airfoils, turbines, and others (Bomela, 2014). Previous work has utilized the geometry of a backward-facing step to consider the partition and the possibility of reattaching the flowing streams. In an alternative model of more perplexing geometries such as airfoils or other three-dimensional shapes, the geometric smoothness of a regressive confronting step stream guarantees the exact purpose of detachment. A large portion of the most punctual investigations of the regressive confronting step

* Correspondence: inb.ali12@atu.edu.iq

¹Department of Power Mechanics, Technical Institute of Babylon, Al-Furat Al Awsat Technical University, Babil, Iraq
Full list of author information is available at the end of the article

streams is tentatively seen in view of stream representation procedures. As a rule, the essential distribution zone was no longer effective, and the outcomes acquired for various geometries are strongly related to the basic stream (Denham & Patrick, 1974; Kumar & Dhiman, 2012). One of the techniques to deal with enhancing separating regions in the confined areas is to use the nanofluids (NFs) (Abchouyeh, Mohebbi, & Fard, 2018; Delouei, Sajjadi, Izadi, & Mohebbi, 2019; Hasan, Sopian, Jaaz, & Al-Shamani, 2017; Izadi, Houghoughi, Mohebbi, & Sheremet, 2018; Izadi, Mohebbi, Chamkha, & Pop, 2018; Izadi, Mohebbi, Karimi, & Sheremet, 2018; Ma, Mohebbi, Rashidi, Yang, & Sheremet, 2019; Mohebbi & Heidari, 2017; Mohebbi & Rashidi, 2017). NFs are those fluids with suspended nanoparticles commonly metal oxides (Saidur, Leong, & Mohammad, 2011) which can be suspended in the base fluid which is commonly water (Yu & Xie, 2012). Along these lines, there is no drop in the stream field. It is found that more testing exhibits that NFs enhance the properties of the heat flux by increasing the flux conductivity and the convective heat transfer coefficients (Al-Aswadi, Mohammed, Shuaib, & Campo, 2010; Al-Shamani et al., 2015; Jaaz et al., 2017; Jaaz, Sopian, & Gaaz, 2018; Ma, Mohebbi, Rashidi, & Yang, 2019; Mohammed, Al-Aswadi, Shuaib, & Saidur, 2011; Mohammed, Al-Aswadi, Yusoff, & Saidur, 2012; Mohebbi, Lakzayi, Sidik, & Japar, 2018; Mohebbi, Nazari, & Kayhani, 2016; Murshed, De Castro, Lourenço, Lopes, & Santos, 2011; Nazari, Mohebbi, & Kayhani, 2014; Sheikholeslami & Ganji, 2016).

The estimation of the flow over a regressive confronting step have been broadly considered in the most recent decades for both constrained and blended convection, see, for instance, Armaly, Durst, Pereira, and Schönung (1983), Gartling (1990), Tylli, Kaitksis, and Ineichen (2002), and subsequent related references therein. Likewise, a few different investigations (Ma, Mohebbi, Rashidi, Manca, & Yang, 2018; Nie & Armaly, 2002; Williams & Baker, 1997) tried the 3-D laminar convection stream in reverse geometrical opposing step. Abu-Mulaweh (2003) led a broad survey of research on laminar blended convection over a backward-facing step (BFS). The reverse confronting step flow while exchanging heat was investigated at uniform wall heat flux and uniform wall temperature variation (Nikkhah et al., 2015; Sheikholeslami & Chamkha, 2016). Blackwell and Armaly (1993) explored various approaches to numerically tackle the issues for consistent 2-D-one-stage blended convection flow in a vertical channel (Selimefendigil & Öztop, 2015).

In another investigation, an exploratory numerical study of a blended convection laminar flow over a regressive

confronting step was performed by Abu-Mulaweh, Armaly, and Chen (1993). Other studies found that the inclination angle influences both the flow and its relevant heat stream fields (Alawi, Azwadi, Kazi, & Abdolbaqi, 2016; Kherbeet et al., 2015; Safaei, Togun, Vafai, Kazi, & Badarudin, 2014). It was concluded that the expansion in the inclination edge from the vertical reduces the adjacent Nu estimation. This expansion is a direct result of a lessening the streamwise caused by the extension of the inclination edge. Hong, Armaly, and Chen (1993) and Iwai, Nakabe, Suzuki, and Matsubara (2000) have anticipated numerically that the laminar blended convection flow over a regressive confronting advance in two-dimensional and three-dimensional configurations, respectively. They observed that the reattachment length increases as the inclination angle increases gradually from 0° to 180° and, hence, a reduction in the wall friction coefficient and Nu was observed (Nazari, Kayhani, & Mohebbi, 2013). The opposite was looked for both reattachment length and Nu as the inclination edge increases from 180° to 360° . Various examinations on turbulent flow over a backward-facing step have been investigated mostly in common and constrained convection; see, for instance (Abe, Kondoh, & Nagano, 1995; Chen, Nie, Armaly, & Hsieh, 2006; Park & Sung, 1995; Rhee & Sung, 1996). A few researchers considered the convective heat flux exchange throughout utilizing NFs, see, for instance, Trisaksri and Wongwises (Daungthongsuk & Wongwises, 2007; Trisaksri & Wongwises, 2007; Wang & Mujumdar, 2007), and the subsequent references therein. It ought to be noted, in any case, that the most investigations of a regressive confronting step employ regular non-NFs (Hashemi, Abouali, & Ahmadi, 2017; Ma, Mohebbi, Rashidi, & Yang, 2018b; Mohammed, Alawi, & Sidik, 2016; Mohammed, Alawi, & Wahid, 2015). Adversely, other investigations with NFs in reverse confronting step geometry have been developed. The primary numerical examination to investigate the stream and heat flux exchange over a regressive confronting step utilizing NFs was performed by Abu-Nada (2008). In this study, the volume fraction nanoparticles (ϕ) and Re were taken at $0 \leq \phi \leq 0.2$ and $200 \leq Re \leq 600$, respectively using the nanoparticles of Al_2O_3 , CuO , SiO_2 , or ZnO . It was suggested that the high Nu number inside the distribution zone generally depends on the thermophysical properties of the nanoparticles (Ma, Mohebbi, Rashidi, Yang, & Sheremet, 2019) while it shows no Re relation (Ma, Mohebbi, Rashidi, & Yang, 2018c).

Numerical examination of forced and mixed convection in even and vertical pipe of various NFs was studied (Al-Aswadi et al., 2010; Mohammed et al., 2011, 2012). The effects of Re number ($75 \leq Re \leq 225$), temperature

difference between 0 and 30 °C using Au, Ag, Al₂O₃, Cu, or CuO as nanoparticles with water as the base fluid were studied, while SiO₂ and TiO₂ were inspected on the fluid stream and heat flux step characteristics. It is found that a dispersion region develops a straight backward-facing step between the edge of the wall and within 1 mm or so before the corner where the downstream divider is located (Alawi et al., 2016). In that couple of millimeters zone between the appropriation region and the downstream divider, the stream shows a reversing U-turn opposing the circulation stream where circulated and uncirculated streams come together in the channel. In these systems, the highest peak of Nu is obtained using Au as the nanoparticle, while the most astonishing slightest peak in the circulation district was obtained using diamond nanoparticles.

The literature review has shown that the steady 2-D-NF laminar mixed convection flowing over a backward-facing step in a vertical configuration under uniform heat flux has not been thoroughly investigated and this case will be a very convincing argument for this study. The present examination, for instance, oversees particular NFs such as CuO, ZnO, and SiO₂ at various volume fractions and various nanoparticle ranges. The impacts of heat flux and Re on the velocity distribution, skin friction coefficient, and Nu are analyzed and offered an explanation to the peak under the effect of NFs on these parameters for facilitating the restricting streams.

The aim is to study the effects of different types of nanoparticles such as Al₂O₃, CuO, SiO₂, and ZnO and base water and to analyze different volume fractions (ϕ) of nanoparticles in the range of 1–4%. The calculations were performed with heat flux, Reynolds numbers (Re), and step height (S) at a range of $100 < Re < 600$, $100 < Re < 500$, and $3 \leq S \leq 5.8$, respectively.

Methodology

Numerical model

Physical model

Figure 1 shows the geometrical arrangement for the direct step backward facing where the two parameters of the stepping height and expansion ratio were set at 4.8 mm and 2, respectively. Additionally, the upstream and downstream walls were assembled at 24 mm and 144 mm, respectively. At the wall, a uniform heat flux (q_w) was applied to the step downstream wall (X_e) while the opposite wall of the channel was kept isothermally consistent with the fluid temperature of T_0 . The wall upstream is characterized by two steps: X_i and S ; both were kept under adiabatic surface condition. The re-attachment length (X_r) is shown on the right side of the

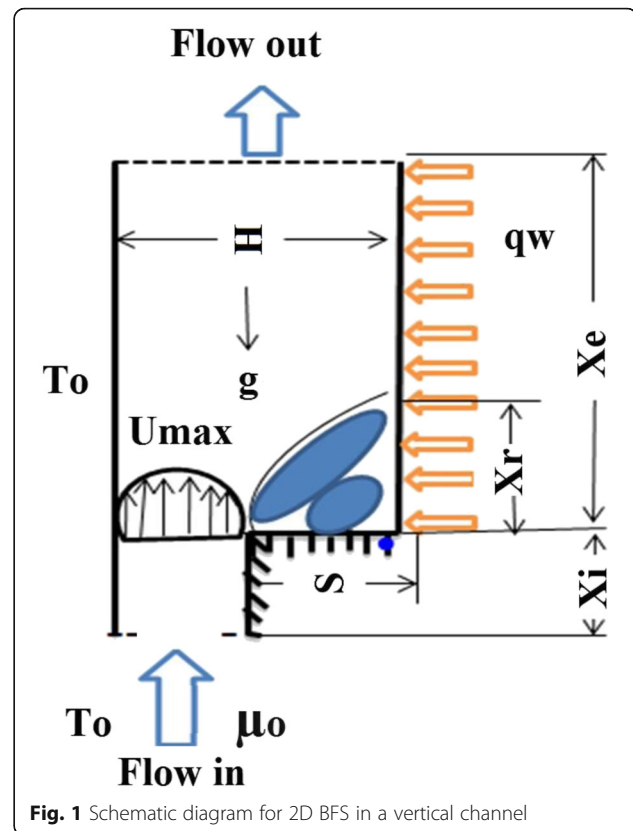


Fig. 1 Schematic diagram for 2D BFS in a vertical channel

bottom of the channel. At the channel entrance, the nanofluid stream is hydrodynamically persistent and the flow achieves the fully developed conditions at the edge of the movement which results in zero speed at the internal surface of the pipe. The nanofluids (nanoparticles and water) were adjusted for specific heat flux to attain a no-slip condition. The flow was assumed to be incompressible and follows Newtonian fluid in regard to the viscosity. As an approximation, the exchange radiation heat flux, its counterpart distribution term, and the inward heat flux were dismissed. The thermophysical properties of the nanofluids are constant while the buoyancy was constrained as an opposing motion to the gravity. The Boussinesq equation is employed for this system.

FLUENT solver is based on the finite volume method. In this case, domain of the model to be examined is discretized into a finite set of the control volumes, which are termed meshes or cells. Then, the general conservation equations for mass, momentum, and energy solved on this set control volumes. Other transport equations such as the equations for species may also be applied. Subsequently, partial differential equations are discretized into a system of algebraic equations. All algebraic equations are solved numerically to render the solution

field. Computational fluid dynamic (CFD) theories, the CFD modeling process, physical model, and assumptions such as model, governing equations and boundary conditions, thermophysical properties of nanofluids, finite volume method (FVM), and fluid computation by the SIMPLE algorithm are presented in the following sections. CFD techniques are used to study and solve complex fluid flow and heat transfer problems in the backward and forward double steps. CFD is a computer-based tool for simulating the behavior of systems involving fluid flow, heat transfer, and other physical-related processes. It works by solving the equations of fluid flow (in a special form) over a region of interest, with specified (known) conditions on the boundary of that region. CFD has facilities in the industry as it can solve several system configurations in the same time and at a cheaper cost compared with other experimental studies. In the current study, a CFD technique is used to investigate the effect of using nanofluids as work fluid instead of the conventional fluids over backward and forward double steps. The interest region where flow simulation is to be done is the computational domain of the problems.

Cost analysis of using nanofluids To investigate the cost-effectiveness of using nanofluids as coolants, computational fluid dynamics method is employed to directly simulate the flow and heat transfer of the nanofluids in a 2-dimensional micro channel in the present paper. There are two different numerical methods for doing these. One is based on molecular dynamics which directly focuses on the molecular behaviors of the nanoparticles. This method needs more CPU time and computer memory. The other is based on Navier-Stokes questions introducing the thermal and dynamic parameters of the nanofluids obtained from the mixture fluid theory and experimental measurements. Nanofluids are prepared by either one-step or two-step methods. Both methods require advanced and sophisticated equipment. This leads to higher production cost of nanofluids. Therefore, high cost of nanofluids is a drawback of nanofluid applications (Xu, Pan, & Yao, 2007).

Governing equations To prepare the CFD investigation of the reverse confronting step, it is imperative to set up the basic three equations which describe the continuity (Eq. 1), momentum (Eq. 2), and the energy (Eq. 3). It is also important to set the non-dimensional variables. In addition, the Boussinesq equation was used to deal with the viscous dispersal and compressibility impact. The conditions for two-dimensional laminar

incompressible streams can be composed as suggested by (Abu-Nada, 2008):

$$\text{The continuity equation : } \frac{\partial U}{\partial X} + \frac{\partial V}{\partial Y} = 0 \quad (1)$$

$$\begin{aligned} X\text{-motion : } U \frac{\partial U}{\partial X} + V \frac{\partial V}{\partial Y} &= -\frac{\partial P}{\partial X} \\ &+ \frac{\mu_{nf}}{\rho_n \nu_{nf}} \frac{1}{Re} \left(\frac{\partial^2 U}{\partial X^2} + \frac{\partial^2 U}{\partial Y^2} \right) \end{aligned}$$

The momentum equations

$$\begin{aligned} Y\text{-motion : } U \frac{\partial U}{\partial X} + V \frac{\partial V}{\partial Y} &= -\frac{\partial P}{\partial Y} \\ &+ \frac{\mu_{nf}}{\rho_n \nu_{nf}} \frac{1}{Re} \left(\frac{\partial^2 U}{\partial X^2} + \frac{\partial^2 U}{\partial Y^2} \right) + \frac{(\rho\beta)_{nf}}{\rho_{nf} \beta_{nf}} \frac{Gr}{Re^2} \theta \end{aligned} \quad (2)$$

$$\text{The energy equation : } U \frac{\partial \theta}{\partial X} + V \frac{\partial \theta}{\partial Y} = \frac{\alpha_{nf}}{\alpha_f Re Pr} \left(\frac{\partial^2 \theta}{\partial X^2} + \frac{\partial^2 \theta}{\partial Y^2} \right) \quad (3)$$

The dimensionless variables are defined as follows,

$$\begin{aligned} X &= \frac{x}{S} \quad Y = \frac{y}{S} \quad \theta = \frac{T - T_0}{T_w - T_0} \\ U &= \frac{u}{U_0} \quad V = \frac{v}{V_0} \quad Re = \frac{\rho u_0 D_h}{\mu} \end{aligned}$$

Boundary conditions The boundary conditions as shown below reflect the limiting situations at the walls in regard to the flow, no-slip condition, and temperature. The conditions at the channel segment include the temperature and the speed. The overall arrangement is governed by the following conditions (Ghasemi & Aminossadati, 2010; Öztop, 2006):

Upstream inlet:

$$X = -\frac{X_i}{D_h} \quad \frac{S}{D_h} \leq Y \leq \frac{H}{D_h} \quad U_1 = \frac{u_i}{u_0} \quad V = 0 \quad \theta = 0$$

Downstream exit:

$$X = \frac{X_e}{D_h} \quad 0 \leq Y \leq \frac{H}{D_h} \quad \frac{\partial^2 U}{\partial X^2} = 0 \quad \frac{\partial^2 V}{\partial X^2} = 0 \quad \frac{\partial^2 \theta}{\partial X^2} = 0$$

Top wall:

$$-\frac{1}{D_h} \leq X \leq \frac{X_e}{D_h} \quad Y = \frac{H}{D_h} \quad U = 0 \quad V = 0 \quad \theta = 0$$

Sidewalls:

$$-\frac{X_i}{D_h} \leq X \leq \frac{X_e}{D_h} \quad 0 \leq Y \leq \frac{H}{D_h} \quad U = 0 \quad V = 0 \quad \theta = 0$$

Stepped wall condition: (a) Upstream:

$$-\frac{X_i}{D_h} \leq X \leq 0 \quad Y = \frac{S}{D_h} \quad U = 0 \quad V = 0 \quad \frac{\partial \theta}{\partial Y} = 0$$

Stepped wall condition: (b) At the step:

$$X = 0 \quad 0 \leq Y \leq \frac{S}{D_h} \quad U = 0 \quad V = 0 \quad \frac{\partial \theta}{\partial Y} = 0$$

Stepped wall condition: (c) Downstream:

$$0 < X \leq \frac{X_i}{D_h} \quad Y = 0 \quad U = 0 \quad V = 0 \quad \frac{\partial \theta}{\partial Y} = -1$$

Code validations and grid testing

- i. Preliminary evaluation of the grid

A preliminary evaluation was adopted to coordinate the grid geometrical conditions and the ability of the grid to show the impact of heat transfer of the fluids with various NFs. The cross investigation was driven with the working fluids, NFs, at $Re = 50$ and 175 , while keeping the downstream wall and the channel stream at temperature difference of $\Delta T = 15$ °C. Three grid size of 140×50 , 128×50 , and 140×60 were used for testing a self-governance system while a fourth grid size of 128×50 was maintained for self-governing independence trials. Several local trials have shown that using other grid sizes reduces the performance of the grid up to 4% in evaluating speed and temperature. The partition between the center points was extended to reach 14 in the x -direction while it reaches 3.5 in the y -direction. The current examination has adopted a non-uniform structure and quadrilateral sides. The system was specifically tested near the steps at the edge and the walls to guarantee the precision of the numerical deviation which helps remarkably to save both the computational time and cross assessment.

The second cross tests have improved the situation of air flow at $Re = 100$ while a uniform heat flux progress of $q_w = 200$ W/m² was applied to the downstream wall. The points of the cross-sectional center are set at different sizes of the grid while the framework numbers in the x -direction were 100, 120, and 140 and 50, 60, and 70 in the y -heading to ensure the system flexibility test. A grid size of 100×50 was used to examine and then to validate the cross self-sufficient course of action. It shows under 3% reduction in Nu and other grid sizes that are mentioned in Table 1, a fine structure is used as a part of the x -coordinate which is close to the divider motion section, while it increases with expansion of 0.1 in x -bearing along the way from the wall position. Other fine grids of the improvement extents at the ratio of 0.285 in the y -heading are utilized very close to the base divider and the edge of the wall to

ensure the accuracy of the framework free course of action.

ii. Validation of the code

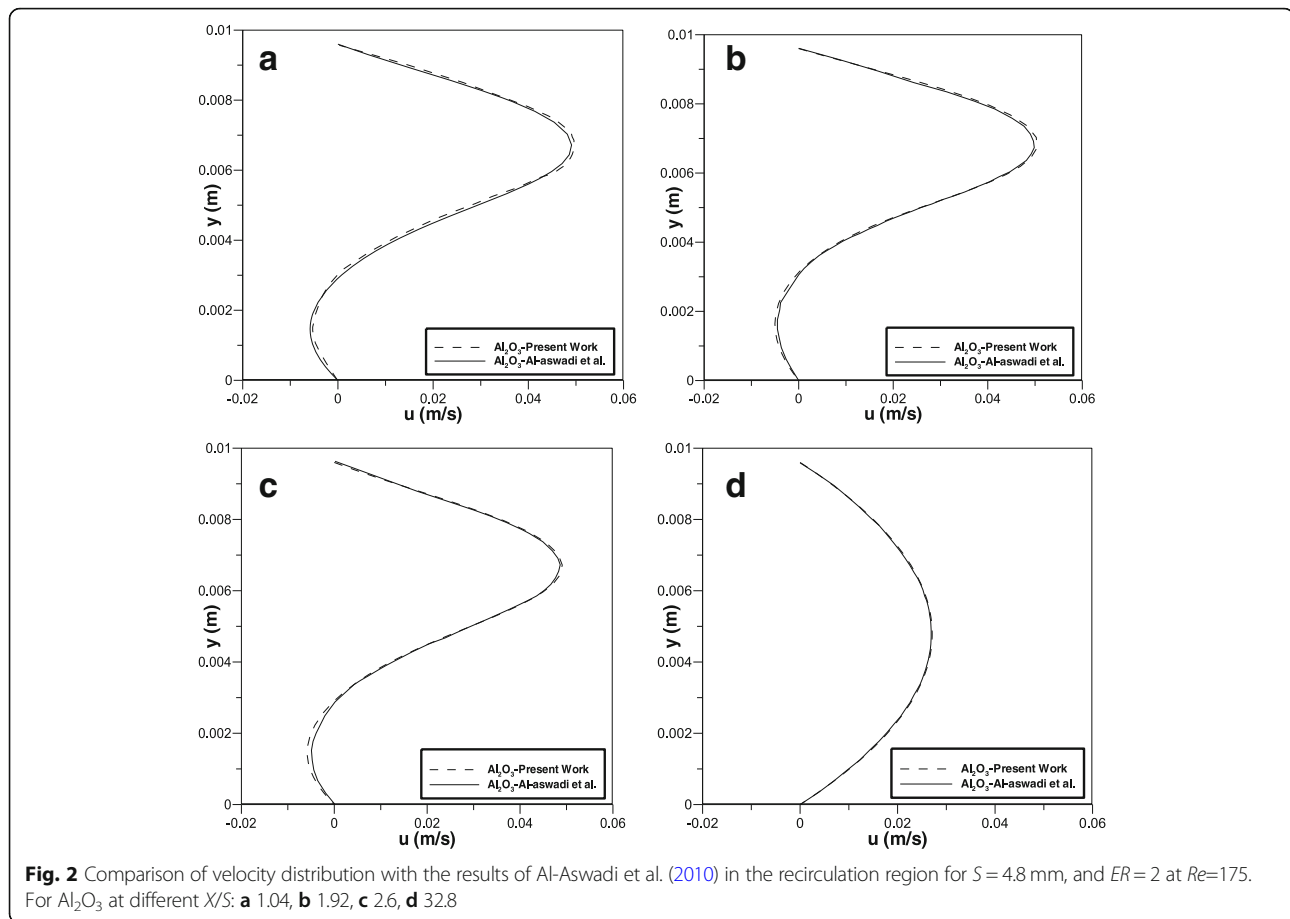
The numerical approval strategy that comprises the numerical code under particular conditions was tested and then used as a benchmark for afterward contrasting. The main experiment was performed by creating the constrained convective nanofluids stream over an even BFS in a pipe (Al-Aswadi et al., 2010). For this stream, Re numbers for the laminar flow were taken at 50 and 175. Figures 2, 3, and 4 demonstrate the consequences of the correlation with the findings of the various NFs as presented by Al-Aswadi et al. (2010). The velocity distribution for different stepped wall increments (X/S) in the distribution along the pipe is shown in Figs. 2 and 3 for Al_2O_3 and CuO under same conditions, respectively. The distribution location shows up and the measure of the local distribution diminishes as the separation between the step X/S achieves the reattachment condition at zero-speed flow as shown in Figs. 2a–d and 3a–d. Figures 2a–c and 3a–c demonstrate that a distribution location grew continuously downstream. Additionally, the downstream of flow begins to end up completely by creating fluid stream toward the pipe exit as shown in Figs. 2 and 3d.

The skin friction coefficients shown in Fig. 4 were demonstrated at the base of the wall step showing that they achieve the separation downstream from the step showing the highest extreme base peak until achieving a consistent friction coefficient along the rest of the base wall. The condition of the flow to reach fully developed flow depends on the asymptotic variation of the skin coefficient. The second experiment was prepared to reproduce blended convective wind stream over BFS in the channel according to the work performed by Hong et al. (1993). The conditions of this experiment include setting Re at 100 and applying a uniform wall heat flux at 200 W/m². The velocity distribution and Nu at the point where $\theta' = 0$ are explained in Fig. 5a, b.

Table 1 Grid tests for the Nusselt number at $Re = 100$

| Grid no. | | Expansion factor (first/last) | | Nusselt number |
|----------------|--------------|-------------------------------|--------------|----------------|
| x -direction | y -heading | x -direction | y -heading | |
| 100 | 50 | 0.1 | 0.285 | 1.75485 |
| | 60 | | | 1.77592 |
| | 70 | | | 1.80250 |
| 120 | 50 | | | 1.75856 |
| | 60 | | | 1.77922 |
| | 70 | | | 1.80828 |
| 140 | 50 | | | 1.76701 |
| | 60 | | | 1.78369 |
| | 70 | | | 1.81702 |

Procedure of numerical calculation The procedure of the numerical calculations was executed through governing equations and the conditions alongside the limit as depicted in Eqs. (1) to (3). The conditions for the strong and fluid stage were considered as a single domain. The discretization of the conditions in the liquid and strong regions has come to an end by utilizing FVM. The diffusion term under energy and momentum conditions is approximated continuously by arranging the focal distinction until achieving a steady state condition. However, a second-arranged upstream procedure was prepared to show the relation to the convective terms. The calculation of the stream field was

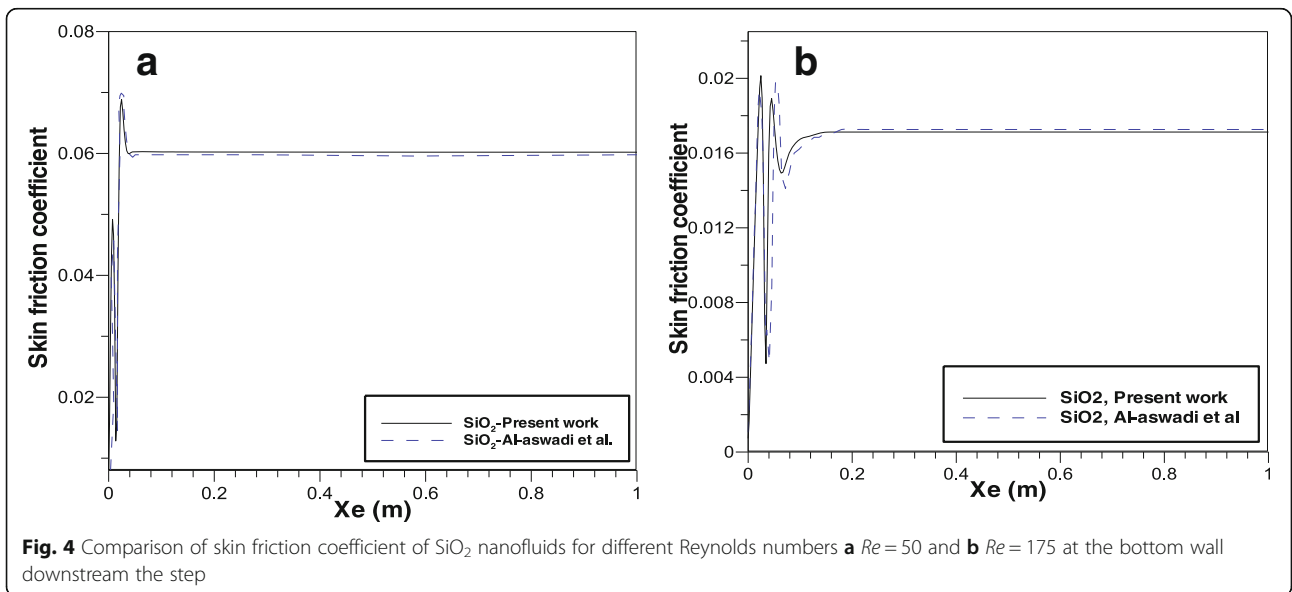
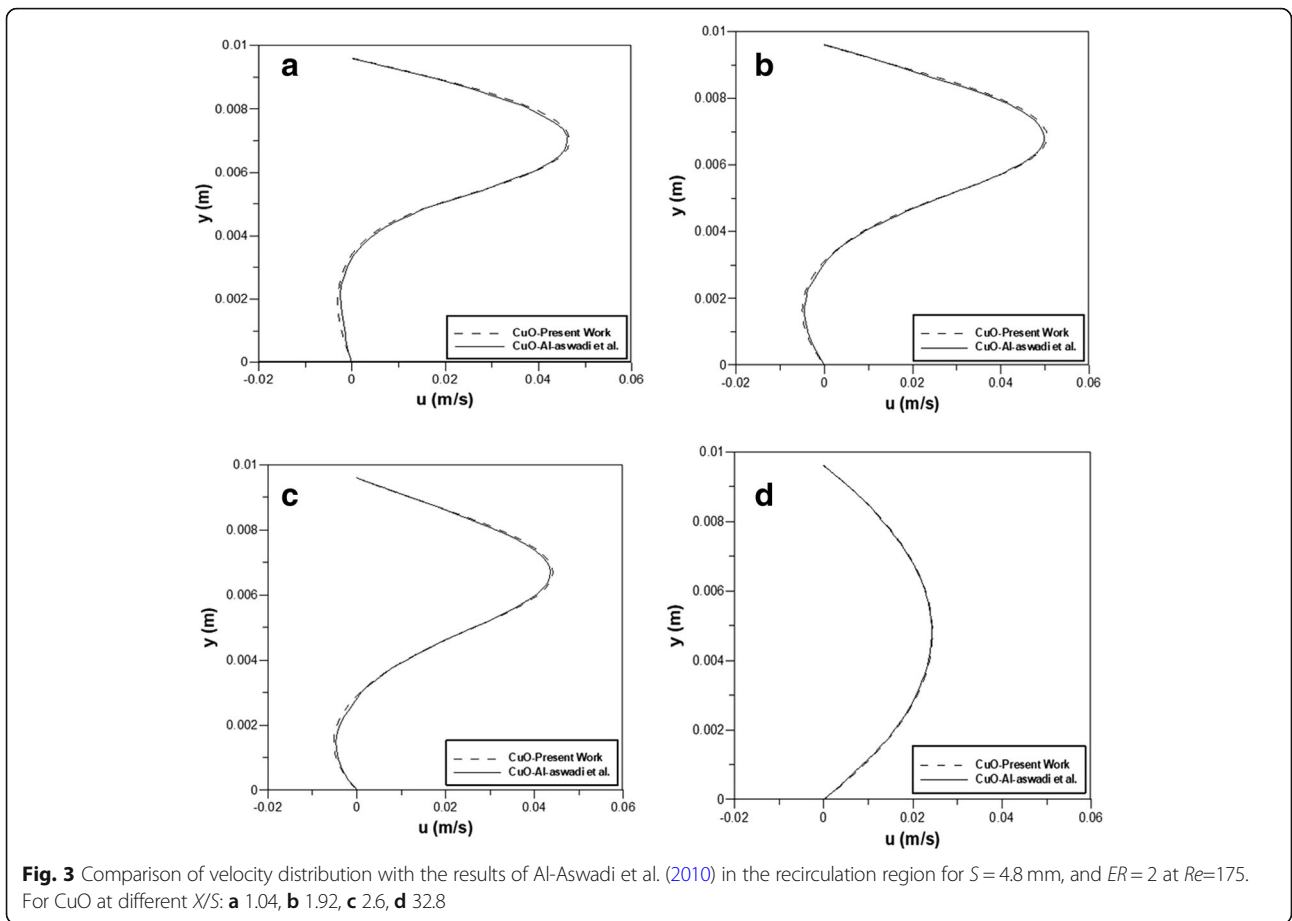


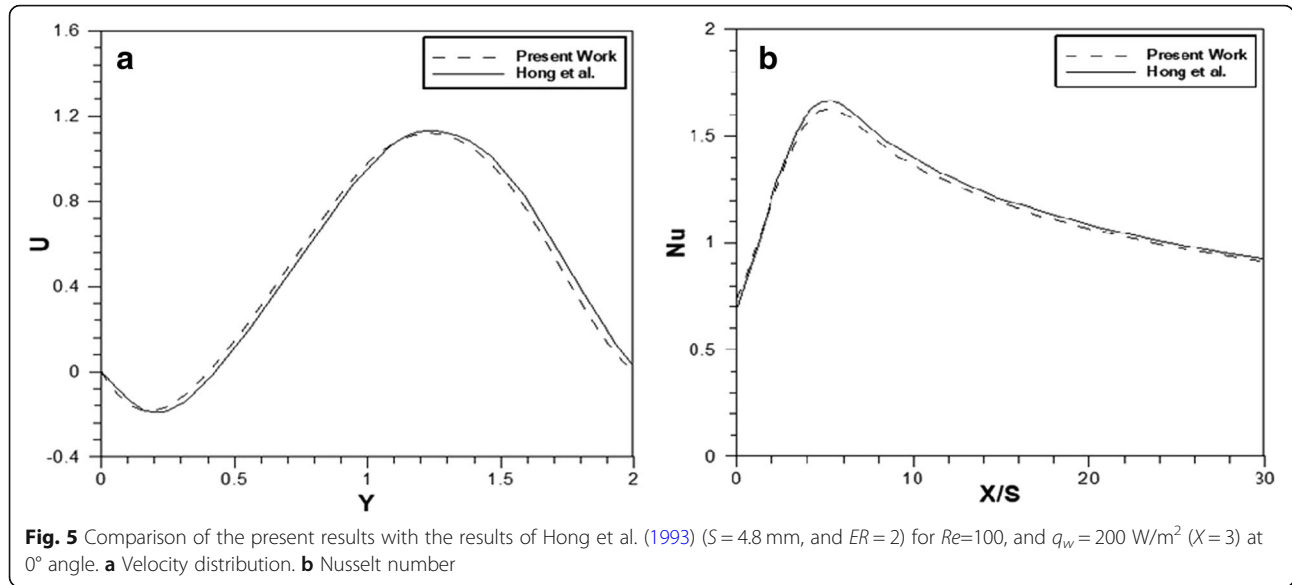
completely utilized by the SIMPLE calculation (John & Anderson, 1995). This was an iterative arrangement methodology where the calculation is introduced through speculating the weight field. At this point, the momentum equations were utilized to determine the speed parts followed by refreshing the weight factor to reach the continuity state. Despite the fact that the steady state does not contain any weight factor, it can be changed effortlessly into a weight adjustment condition (Patanker, 1980).

Thermophysical characteristics of nanofluids The zinc oxide (ZnO) nanoparticles were synthesized using a simple precipitation method with zinc sulfate and sodium hydroxide as starting materials. The synthesized sample was calcined at different temperatures for 2 h (Kumar, Venkateswarlu, Rao, & Rao, 2013); copper oxide (CuO) is the inorganic compound with the formula CuO. As a black solid, it is one of the two stable oxides of copper, the other being Cu_2O or cuprous oxide. As a mineral, it is known as tenorite. It is a product of copper mining and the precursor to many other copper-containing products and chemical compounds (Richardson, 2002). Silicon dioxide (SiO_2), also known as silica, is an oxide of silicon with the chemical formula SiO_2 , most commonly found in

nature as quartz and in various living organisms (Fernández, Lara, & Mitchell, 2015; Iler, 1979). In many parts of the world, silica is the major constituent of sand. Silica is one of the most complex and most abundant families of materials, existing as a compound of several minerals and as a synthetic product. Notable examples include fused quartz, fumed silica, silica gel, and aerogels. It is used in structural materials and microelectronics (as an electrical insulator) and as components in the food and pharmaceutical industries. Aluminium oxide (Al_2O_3) (IUPAC name) or aluminum oxide (American English) is a chemical compound of aluminum and oxygen with the chemical formula (Al_2O_3). It is the most commonly occurring of several aluminum oxides and specifically identified as aluminum (III) oxide. It is commonly called alumina and may also be called aloxide, aloxite, or alundum depending on particular forms or applications. It occurs naturally in its crystalline polymorphic phase $\alpha-Al_2O_3$ as the mineral corundum, varieties of which form the precious gemstones ruby and sapphire. Al_2O_3 is significant in its use to produce aluminum metal, as an abrasive owing to its hardness and as a refractory material owing to its high melting point (Davis, 1993).

With a specific end goal to complete simulation for NFs, the compelling thermophysical characteristics of





NFs must be first determined. For this situation, the nanoparticles are Al₂O₃, CaO, ZnO, and SiO₂. The required properties for the recreations are to set the effective heat conductivity (k_{eff}), to calculate the effective viscosity (μ_{eff}) and effective density (ρ_{eff}), and to assume that the effective coefficient of heat expansion (β_{eff}) and effective particular heat capacity (c_{peff}) are following the incompressible fluid and their estimation depends on the volume fraction of their nanofluid (ϕ). By utilizing Brownian movement of nanoparticles in reverse confronting step, the effective heat flux conductivity can be acquired as following mean experimental requirements (Ghasemi & Aminossadati, 2010; Heidari, Mohebbi, & Safarzade, 2016):

$$k_{eff} = k_{static} + k_{Brownian} \tag{4}$$

where k_{static} is defined as,

$$k_{static} = k_{bf} \left[\frac{k_{np} + 2k_{bf} - 2(k_{bf} - k_{np})\phi}{k_{np} + 2k_{bf} + 2(k_{bf} - k_{np})\phi} \right] \tag{4.1}$$

and the Brownian thermal conductivity,

$$k_{Brownian} = 5 \times 10^4 \beta \phi c_{p,bf} \sqrt{\frac{kT}{2\rho_{np}R_{np}}} f(T, \phi) \tag{4.2}$$

where Boltzmann constant:

$$k = 1.3807 \times 10^{-23} \text{ J/K}$$

$$\beta_{Al_2O_3} = 8.4407(100\phi)^{-1.07304}$$

$$\beta_{CuO} = 9.881(100\phi)^{-0.9446}$$

Modeling function, β (Vajjha & Das, 2009):

$$\beta_{SiO_2} = 1.9526(100\phi)^{-1.4594}$$

$$\beta_{ZnO} = 8.4407(100\phi)^{-1.07304}$$

Modeling function

$$f(T, \phi) = (2.8217 \times 10^{-2}\phi) + 3.917 \times 10^{-3} \left(\frac{T}{T_0} \right) + (-3.0699 \times 10^{-2}\phi - 3.91123 \times 10^{-3})$$

and μ_{eff} can be empirically estimated (Corcione, 2010):

$$\mu_{eff} = \frac{\mu_f}{1 - 34.87 \left(\frac{d_p}{d_f} \right)^{-0.3} \phi^{1.03}} \tag{5}$$

where,

$$\text{The equivalent diameter is } d_{eff} = \left(\frac{6M}{N\pi\rho_{bt}} \right)^{1/3} \tag{6}$$

$$\text{The density of NF [68] is } \rho_{nf} = (1 - \phi)\rho_f + \phi\rho_{np} \tag{7}$$

The effective heat capacity at constant pressure of NF (Ghasemi & Aminossadati, 2010) is:

$$(c_p)_{nf} = (1 - \phi)(c_p)_f + \phi(c_p)_{np} \tag{8}$$

The effective coefficient of thermal expansion of nanofluid (Ghasemi & Aminossadati, 2010):

$$(\beta)_{nf} = (1 - \phi)(\beta)_f + \phi(\beta)_{np} \tag{9}$$

The experimental values of the thermophysical properties for pure water with different NFs at 300 K are listed in Table 2.

Table 2 Thermophysical properties for pure water and different nanofluids at $T = 300$ K (Corcione, 2010)

| Thermophysical properties | Water | Al ₂ O ₃ | CuO | ZnO | SiO ₂ |
|---|-----------------------|--------------------------------|----------------------|----------------------|----------------------|
| Density, ρ (kg/m ³) | 998.203 | 3970 | 6500 | 5600 | 2200 |
| Dynamic viscosity, μ (Ns/m ²) | 2.01×10^{-3} | – | – | – | – |
| Thermal conductivity, k (W/m K) | 0.613 | 40 | 20 | 13 | 1.2 |
| Specific heat, C_p (J/kg K) | 4182.2 | 765 | 535.6 | 495.2 | 703 |
| Coefficient of thermal expansion, β (1/K) | 2.06×10^{-4} | 5.8×10^{-6} | 4.3×10^{-6} | 4.3×10^{-6} | 5.5×10^{-6} |

Results and discussion

Reattachment zone

The zone was allocated to display the numerical results to test the 2-D vertical mixed convective stream by standing up the step. The results of speed distribution and skin friction coefficient were taken at different values of Nu at various nanofluids at hand, various nanoparticle volume fractions, Reynolds numbers, and varying heat flux and the height of the wall, and finally with varying nanoparticle diameters. The Reynolds number was taken between 100 and 500 while the heat flux was considered between 100 and 600 W/m². The stream reaches out from a totally developed upstream to outline a basic circulation region. Starting forward, the speed profile is reattached and redeveloped pushing toward a totally developed stream as fluid streams toward channels exit.

Nanofluid parameters' impacts

The nanoparticles with water as a base fluid of Al₂O₃, CaO, ZnO, and SiO₂ were used. The impact of various nanofluids on the heat transfer enhancement was tested under the following parameters of $\phi = 0.04$, $d_p = 25$ nm, $Re = 100$, and $q_w = 500$ W/m² along the channel. Figure 6a shows that Nu acquires the highest value near the wall due to an increasing heating of the wall which decreases steadily as the detachment continues. This is a result of the temperature refinement when the exchanged stream is joined to the essential separated stream which

has a lower temperature. It is found that SiO₂ nanofluid has the highest Nu peak followed by Al₂O₃, CuO, and finally ZnO. The results mentioned can be explained in terms of how much is the reduction in the fluid viscosity and the effect of the heat flux since the viscosity is very critical to these two factors.

This study also shows the effect of ϕ between 1 and 4% on the characteristics of the heat transfer as illustrated in Fig. 6b under the conditions of nanoparticle $d_p = 25$ nm, $Re = 100$, and $q_w = 500$ W/m². As ϕ increases, the Nu of SiO₂ nanofluids ends up higher than that of unadulterated fluids. This is because of the density increasing which prompts the heat transfer enhancement as showed in Fig. 6b. A possible explanation to this could be referred to the effect of the decreasing temperature refinement as ϕ increases which results in increasing the heat transfer improvement. The impact of the diameter of nanoparticles on the heat transfer reveals that the heat transfer varies significantly with the mean nanoparticle diameter between 25 and 80 nm, at $Re = 100$, $\phi = 4\%$, and $q_w = 500$ W/m².

Figure 6c shows the eventual outcome of Nu when SiO₂ nanofluids were used. It has been shown that the mean nanofluid diameter increases due to the increasing Nu . This is because the nanofluid properties such as density and heat capacity increase with a decreasing nanoparticle volume ratio which affects the surface area. Thus, the small diameter of the nanoparticles results in increasing the heat transfer improvement. Consequently,

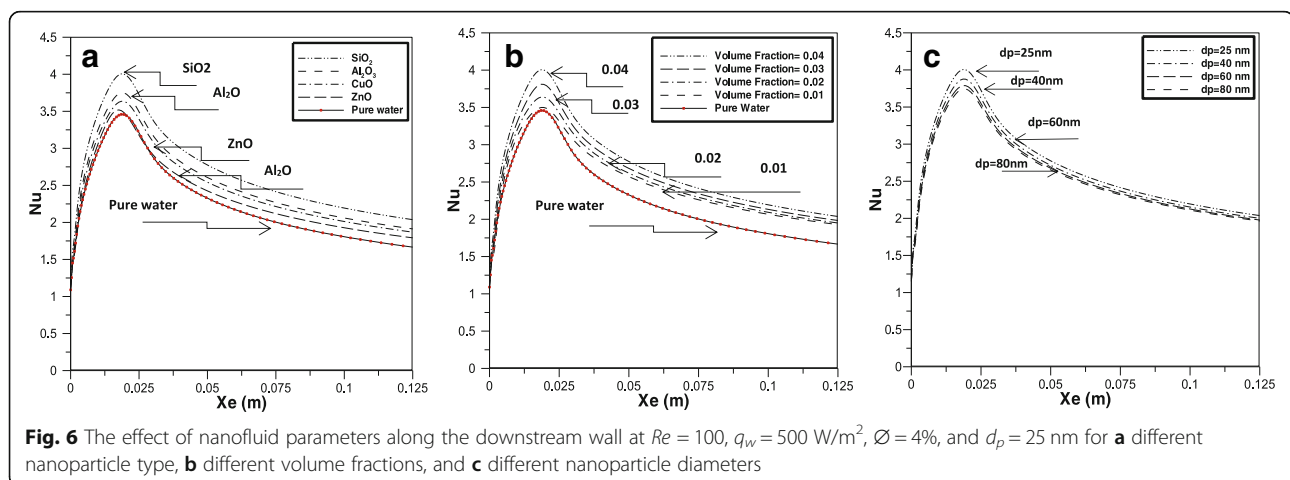


Fig. 6 The effect of nanofluid parameters along the downstream wall at $Re = 100$, $q_w = 500$ W/m², $\phi = 4\%$, and $d_p = 25$ nm for **a** different nanoparticle type, **b** different volume fractions, and **c** different nanoparticle diameters

Nu increases as the diameter of the nanoparticles increases.

Different Reynolds numbers' impacts

Distribution of the velocity

Figure 7 shows the speed circulations of SiO_2 nanofluid at Re numbers in the scope of $100 \leq Re \leq 500$, $q_w = 500 \text{ W/m}^2$, $d_p = 25 \text{ nm}$, and $\varnothing = 4\%$ at various X/S sections along the stepped wall. In Fig. 7a, as Re increases, the speed profile for SiO_2 nanofluid becomes more profound and illustrative. The speed increases as Re increases until reaching the distribution at which the flow reached the reattachment. It has been noted that as the separation between the step and the stepped wall increase, the flow achieves the reattachment faster and the span of the distribution area diminishes as Re expands further as shown in Fig. 7b, c. Beyond this point, the downstream shows that the flow begins to redevelop until reaching completely developed flow at the exit as shown in Fig. 7d.

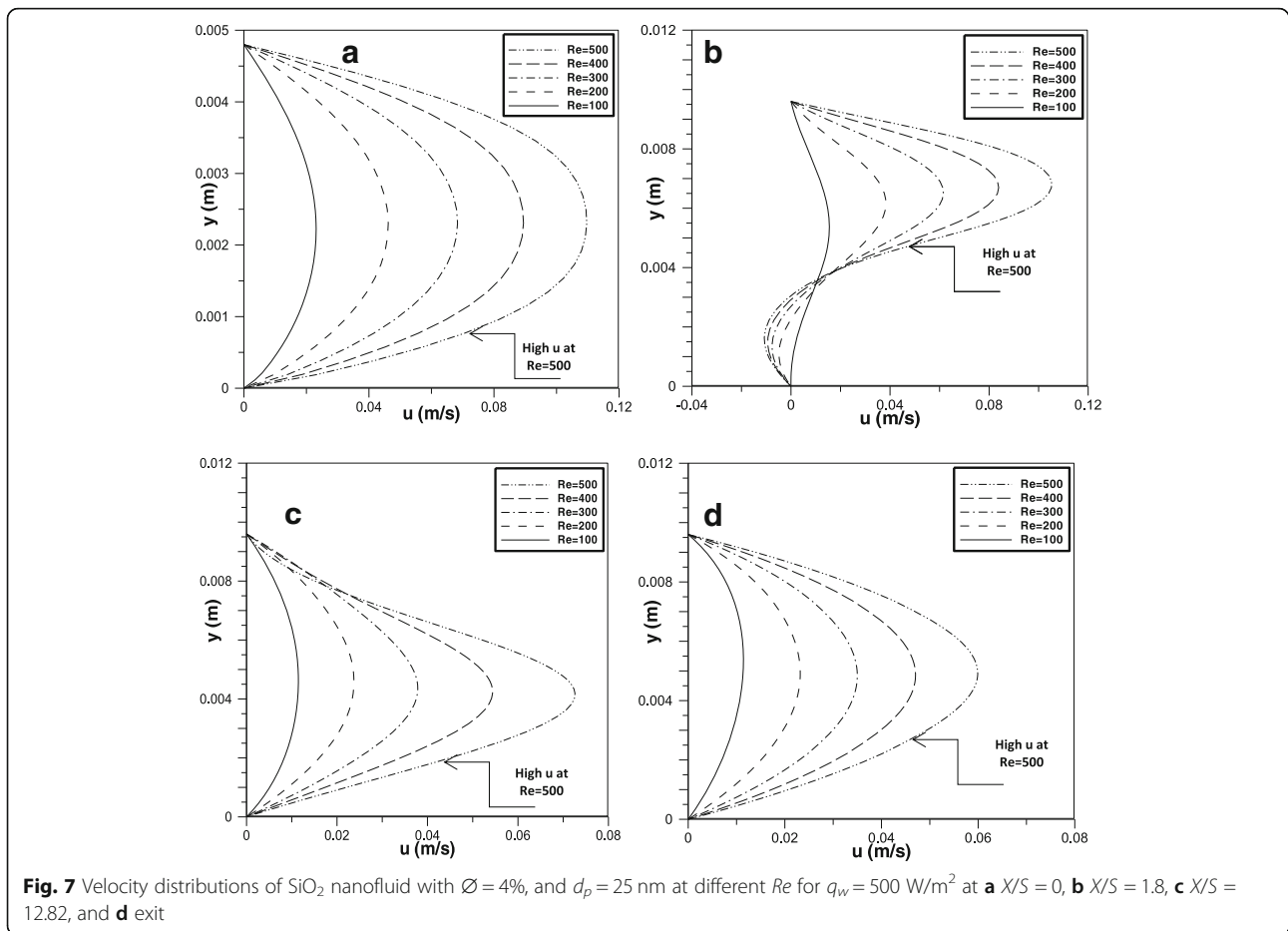
Coefficient of skin friction

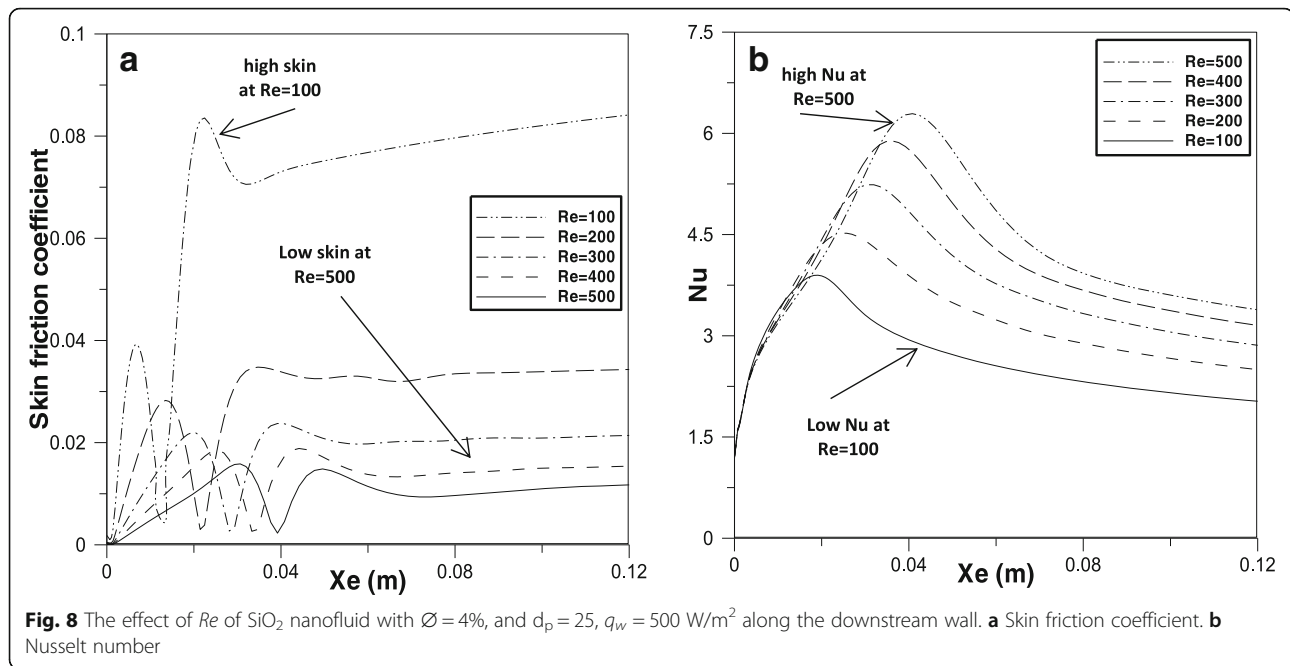
Figure 8a explains the behavior of the skin friction coefficient of the SiO_2 nanofluid at Re in the scope of

$100 \leq Re \leq 500$, $\varnothing = 4\%$, $q_w = 500 \text{ W/m}^2$, and $d_p = 25 \text{ nm}$ along the downstream wall. It is shown that the skin friction coefficient decreases rapidly as Re increases. Additionally, it is seen that the crests at and close to the essential local distribution are displaced along the way from the wall divider in the streamwise bearing as Re increases. This increase comes with the increasing of the length differential of the essential distribution region. The behavior of the coefficient of friction is inversely proportional.

Nusselt number

The Nu of SiO_2 nanofluid at Re between 100 and 500, $\varnothing = 4\%$, $q_w = 500 \text{ W/m}^2$, and $d_p = 25 \text{ nm}$ along the downstream wall is plotted in Fig. 8b. It is shown that Nu increases as Re increases exhibiting stronger convective current which is caused by the reduction in the isotherms. The behavior of Nu shows an exponential reduction from its optimal level until the vortex is started forming. At the highest Re , the stream decreases to the minimum apex of the Nu number at the region where the flows are mixed. Along this zone, the Nu SiO_2 nanofluid was found to possess higher values as Re number increases.





Various heat fluxes' impacts

Distribution of the velocity

Figure 9 shows the speed distribution of SiO_2 nanofluid at q_w varies between 100 and 600 W/m^2 , $Re = 100$, $d_p = 25$ nm, and $\phi = 4\%$ along the X/S sections. It seems that there is an insignificant effect at the edge region, as the stream profiles show no pattern difference as shown in Fig. 9a.

However, the degree of the circulation area expands as the heat transfer increases between the heated stepped wall and the stream of the nanofluid as shown in Fig. 9b, c. It was also found that the buoyancy force slightly pushes up the fast stream and cutting down heat flux and increasing the reattachment length. As the divisions, X/S along the wall increases the circulation zone decreases as shown in Fig. 9b, c. At this location, the flow starts to redevelop approaching full developing stream flow at the exit according to Fig. 9d.

Skin friction coefficient

The testing of the skin friction of SiO_2 nanofluid was carried out with $\phi = 4\%$, and $d_p = 25$ nm, heat flux in the scope of $100 \ll q_w \ll 600 \text{ W/m}^2$, and $Re = 100$ along the downstream divider are shown in Fig. 10a. It is observed that the increase in the heat flow enhances the skin friction coefficient. However, at a particular heat flux of $q_w = 600 \text{ W/m}^2$, the skin friction coefficient shows higher values due to the diminishing shear stress at the vortex.

Nusselt number

Figure 10b explains the behavior of Nu - SiO_2 with $\phi = 4\%$, $d_p = 25$ nm, heat flux of $100 \ll q_w \ll 600 \text{ W/m}^2$, and

$Re = 100$ along the downstream divider. As q_w increases, it was noticed that the highest value of Nu decreases due to the increasing effect of the expanding buoyancy force.

It is important to note that the reduction of optimized Nu continues until roughly the exiting point. The results show that the stream with high heat flow possesses the most astounding Nu least peak in the region where the flows are mixed. It was also found that alongside this territory, Nu with SiO_2 nanofluid possesses the highest value when the heat flow is at the highest value.

Conclusions

Numerical simulation for laminar blended convection stream in a vertical 2-D backward-facing step channel configuration was investigated under a variety of parameters and initial conditions. This topic has recently gained special importance especially due to consolidating Re and nanofluids such as aluminum, copper(II) oxide, zinc oxide, and silicon dioxide with water. Reynolds number was chosen within $100 \ll Re \leq 500$, diameter of nanoparticles d_p : [25, 80] nm, and ϕ : [1%, 4%]. The backward-facing step downstream flow has reached its uniform condition at the uniform heat flux between 100 and 600 W/m^2 while the channel particular propel statuses were taken in the extent of $3.0 \ll S \ll 5.8$ mm. The governing equations have shown very good agreement with the solution using FVM with specific suppositions coupled with proper limit conditions. The current investigation examined the influence of the stream and its relevant opposing flow on the properties of the heat flux. The following conclusions are drawn from this investigation:

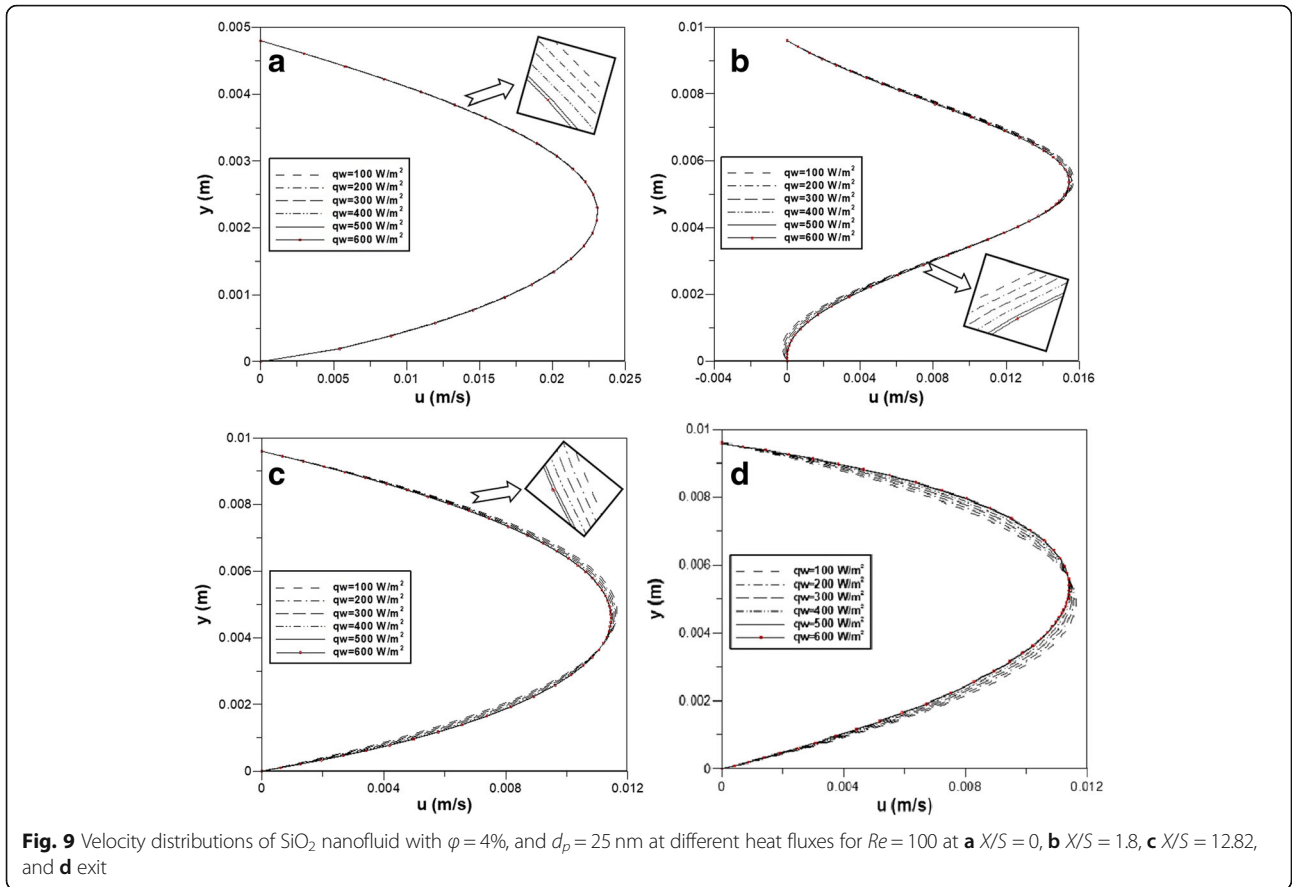


Fig. 9 Velocity distributions of SiO_2 nanofluid with $\phi = 4\%$, and $d_p = 25$ nm at different heat fluxes for $Re = 100$ at **a** $X/S = 0$, **b** $X/S = 1.8$, **c** $X/S = 12.82$, and **d** exit

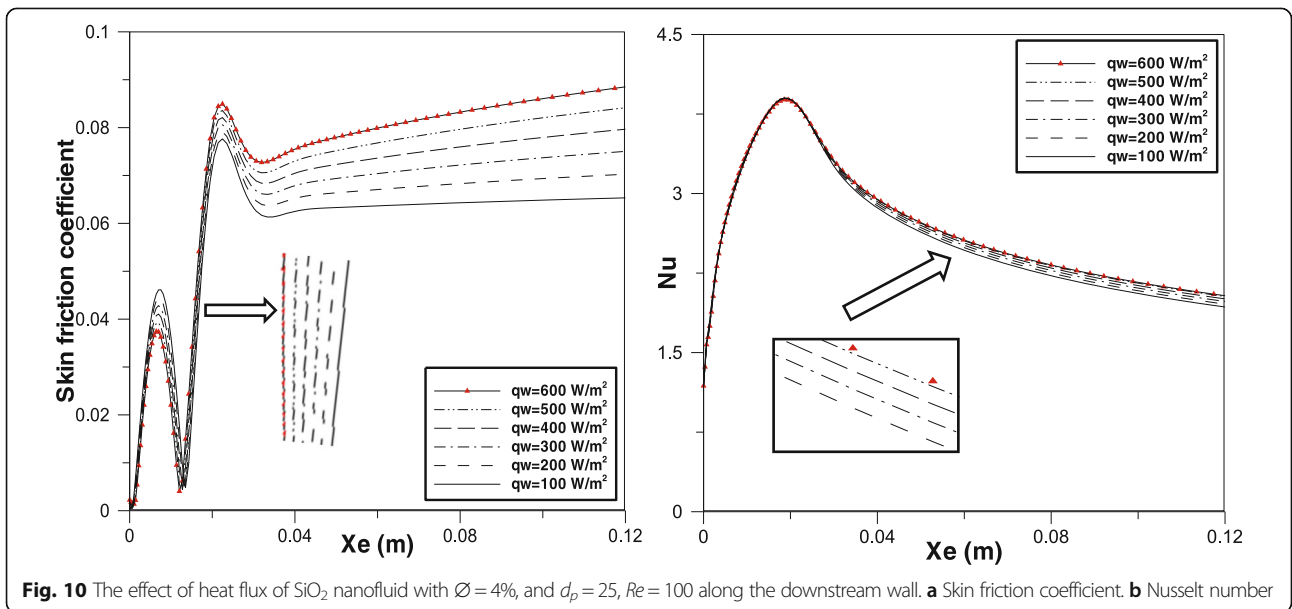


Fig. 10 The effect of heat flux of SiO_2 nanofluid with $\phi = 4\%$, and $d_p = 25$, $Re = 100$ along the downstream wall. **a** Skin friction coefficient. **b** Nusselt number

1. SiO₂ nanoparticles show the most astounding Nu followed by Al₂O₃, CaO, and ZnO.
2. Nu increased continuously by expanding Re and by increasing the step height as well. It was also observed that Nu increases as the heat flux increases. However, Nu is slowly diminishing as the nanofraction diminishes.
3. The present work creates a region of a straight downstream distribution for blended convection stream at various Re and heat flux. It was found that this distribution is highly dependent on increasing Re . The best location of this distributing region was allocated at the interface of the corner where the stepping height joins the downstream wall.
4. The heat flux was found very dependent on the conditions that correlate the preferred flux exchange rate over restricting stream condition.

Nomenclature

A Area (m²)
 Al₂O₃ Aluminum oxide
 A_r Aspect ratio
 BFS Backward-facing step
 c_p Specific heat (kJ/kg K)
 CFD Computational fluid dynamic
 CuO Copper oxide
 d_p Diameter of nanofluid particles (nm)
 FVM Finite volume method
 D_h Hydraulic diameter at inlet (m)
 ER Expansion ratio, H/S
 e Expansion successive ratio
 FFS Forward-facing step
 f Elliptic relaxation function
 Gr Grashof number, gβΔTS³/ν²
 g Gravitational acceleration (m/s²)
 H Total channel height (m)
 h Inlet channel height (m)
 h Convective heat transfer coefficient (W/m² K)
 H₂O Water
 k Thermal conductivity (W/m K)
 k Turbulent kinetic energy (m²/s²)
 S Step height (m)
 SiO₂ Silicon dioxide
 L Total length channel (m)
 Nu Nusselt number, hs/k
 Nu_{s, max} Maximum Nusselt number, hs/k
 P Nodal point number of processors
 p Pressure (p_a)
 p_a Pressure at the outlet (p_a)
 Pr Prandtl number, μ C_p/k
 q_w Wall heat flux (W/m²)
 Re Reynolds number, ρu_o D_h/μ
 Ri Richardson number, Gr/Re²

T Temperature (K)
 T_w Heat wall temperature (K)
 T_o Temperature at the inlet, outlet, or top wall (K)
 UHF Uniform heat flux
 U Dimensionless streamwise velocity component, u/u_o
 u Velocity component x-direction (m/s)
 u_o Average velocity for inlet flow (m/s)
 u_∞ Free-stream velocity (m/s)
 V Dimensionless transverse velocity component, v/u_o
 v Velocity component y-direction (m/s)
 X Dimensionless length at x-coordinate, x/S
 x x-Coordinate direction (m)
 X_e Downstream wall length (m)
 X_i Upstream wall length (m)
 X_n Nusselt number peak length (m)
 X_o Secondary recirculation length (m)
 X_r Reattachment length (m)
 Y Dimensionless length at y-coordinate, y/S
 y y-Coordinate direction (m)
 ZnO Zinc oxide

Greek symbols

ρ Density (kg/m³)
 β Thermal expansion coefficient, (1/K)
 ν Kinematic viscosity (m²/s)
 φ Volume fraction (%)
 μ Dynamic viscosity (N m/s)
 α Thermal diffusivity of the fluid (m²/s)
 Δ Amount of difference
 Dimensionless temperature, (T - T_o)/(T_w - T_o)

Subscripts

bf Base fluid
 i Inlet
 o Outlet
 f Fluid
 nf Nanofluid
 s Solid (nanoparticles)
 W Wall

Acknowledgements

The authors gratefully acknowledge the Al-Furat Al Awsat Technical University 'Iraq' for supporting this work.

Authors' contributions

AAA-O and AJC carried out the experiments. ARY, MHM, and DHA collected the data and did the validation. AAH and MST supervised the project. AAA wrote the manuscript with support from TSG. All authors read and approved the final manuscript.

Funding

UKM-YSD Grant 020-2017

Availability of data and materials

All data generated or analyzed during this study are included in this published article.

Competing interests

The authors declare that they have no competing interests.

Author details

¹Department of Power Mechanics, Technical Institute of Babylon, Al-Furat Al Awsat Technical University, Babil, Iraq. ²Technical College Al-Musaib, Al-Furat Al Awsat Technical University, Al-Musaib, Babil 51009, Iraq. ³Faculty of Engineering & Built Environment, Universiti Kebangsaan Malaysia, 43600 Bangi, Selangor, Malaysia. ⁴Energy and Renewable Energies Technology Center, University of Technology, Baghdad 10001, Iraq.

Received: 8 March 2019 Accepted: 8 July 2019

Published online: 18 September 2019

References

- Abchouyeh, M. A., Mohebbi, R., & Fard, O. S. (2018). Lattice Boltzmann simulation of nanofluid natural convection heat transfer in a channel with a sinusoidal obstacle. *International Journal of Modern Physics C*, 29, 1850079.
- Abe, K., Kondoh, T., & Nagano, Y. (1995). A new turbulence model for predicting fluid flow and heat transfer in separating and reattaching flows—II. Thermal field calculations. *International Journal of Heat and Mass Transfer*, 38, 1467–1481.
- Abu-Mulaweh, H. (2003). A review of research on laminar mixed convection flow over backward-and forward-facing steps. *International Journal of Thermal Sciences*, 42, 897–909.
- Abu-Mulaweh, H., Armaly, B. F., & Chen, T. (1993). Measurements of laminar mixed convection in boundary-layer flow over horizontal and inclined backward-facing steps. *International Journal of Heat and Mass Transfer*, 36, 1883–1895.
- Abu-Nada, E. (2008). Application of nanofluids for heat transfer enhancement of separated flows encountered in a backward facing step. *International Journal of Heat and Fluid Flow*, 29, 242–249.
- Al-Aswadi, A., Mohammed, H., Shuaib, N., & Campo, A. (2010). Laminar forced convection flow over a backward facing step using nanofluids. *International Communications in Heat and Mass Transfer*, 37, 950–957.
- Alawi, O., Azwadi, C. N., Kazi, S., & Abdolbaqi, M. K. (2016). Comparative study on heat transfer enhancement and nanofluids flow over backward and forward facing steps. *Journal of Advanced Research in Fluid Mechanics and Thermal Sciences*, 23, 25–49.
- Al-Shamani, A. N., Sopian, K., Mohammed, H., Mat, S., Ruslan, M. H., & Abed, A. M. (2015). Enhancement heat transfer characteristics in the channel with trapezoidal rib-groove using nanofluids. *Case Studies in Thermal Engineering*, 5, 48–58.
- Armaly, B. F., Durst, F., Pereira, J., & Schönung, B. (1983). Experimental and theoretical investigation of backward-facing step flow. *Journal of Fluid Mechanics*, 127, 473–496.
- Blackwell, B., & Armaly, B. (1993). Computational aspects of heat transfer benchmark problems. *ASME HTD*, 258, 1–10.
- Bomela, C. L. (2014). *The effects of inlet temperature and turbulence characteristics on the flow development inside a gas turbine exhaust diffuser*. Charlotte: The University of North Carolina.
- Chen, Y., Nie, J., Armaly, B., & Hsieh, H.-T. (2006). Turbulent separated convection flow adjacent to backward-facing step—effects of step height. *International Journal of Heat and Mass Transfer*, 49, 3670–3680.
- Corcione, M. (2010). Heat transfer features of buoyancy-driven nanofluids inside rectangular enclosures differentially heated at the sidewalls. *International Journal of Thermal Sciences*, 49, 1536–1546.
- D'Adamo, J., Sosa, R., & Artana, G. (2014). Active control of a backward facing step flow with plasma actuators. *Journal of Fluids Engineering*, 136, 121105.
- Daunghthongsuk, W., & Wongwises, S. (2007). A critical review of convective heat transfer of nanofluids. *Renewable and Sustainable Energy Reviews*, 11, 797–817.
- Davis, J. R. (1993). *Aluminum and aluminum alloys: ASM international*.
- Delouei, A. A., Sajjadi, H., Izadi, M., & Mohebbi, R. (2019). The simultaneous effects of nanoparticles and ultrasonic vibration on inlet turbulent flow: an experimental study. *Applied Thermal Engineering*, 146, 268–277.
- Denham, M., & Patrick, M. (1974). Laminar flow over a downstream-facing step in a two-dimensional flow channel. *Transactions of the Institution of Chemical Engineers*, 52, 361–367.
- Fernández, L. D., Lara, E., & Mitchell, E. A. (2015). Checklist, diversity and distribution of testate amoebae in Chile. *European Journal of Protistology*, 51, 409–424.
- Gartling, D. K. (1990). A test problem for outflow boundary conditions—Flow over a backward-facing step. *International Journal for Numerical Methods in Fluids*, 11, 953–967.
- Ghasemi, B., & Aminossadati, S. (2010). Brownian motion of nanoparticles in a triangular enclosure with natural convection. *International Journal of Thermal Sciences*, 49, 931–940.
- Hasan, H. A., Sopian, K., Jaaz, A. H., & Al-Shamani, A. N. (2017). Experimental investigation of jet array nanofluids impingement in photovoltaic/thermal collector. *Solar Energy*, 144, 321–334.
- Hashemi, Z., Abouali, O., & Ahmadi, G. (2017). Direct numerical simulation of particle–fluid interactions: a review. *Iranian Journal of Science and Technology, Transactions of Mechanical Engineering*, 41, 71–89.
- Hashim, W. M., Shomran, A. T., Jurmut, H. A., Gaaz, T. S., Kadhum, A. A. H., & Al-Amieri, A. A. (2018). Case study on solar water heating for flat plate collector. *Case Studies in Thermal Engineering*, 12, 666–671.
- Heidari, H., Mohebbi, R., & Safarzade, A. (2016). Parameter estimation in fractional convection-diffusion equation. *PONTE International Scientific Research Journal*, 72, 55–68.
- Hong, B., Armaly, B. F., & Chen, T. (1993). Laminar mixed convection in a duct with a backward-facing step: The effects of inclination angle and Prandtl number. *International Journal of Heat and Mass Transfer*, 36, 3059–3067.
- Iler, R. K. (1979). *The chemistry of silica* (pp. 30–62). New York: Wiley.
- Iwai, H., Nakabe, K., Suzuki, K., & Matsubara, K. (2000). The effects of duct inclination angle on laminar mixed convective flows over a backward-facing step. *International Journal of Heat and Mass Transfer*, 43, 473–485.
- Izadi, M., Hoghoughi, G., Mohebbi, R., & Sheremet, M. (2018). Nanoparticle migration and natural convection heat transfer of Cu-water nanofluid inside a porous undulant-wall enclosure using LTNE and two-phase model. *Journal of Molecular Liquids*, 261, 357–372.
- Izadi, M., Mohebbi, R., Chamkha, A., & Pop, I. (2018). Effects of cavity and heat source aspect ratios on natural convection of a nanofluid in a C-shaped cavity using Lattice Boltzmann method. *International Journal of Numerical Methods for Heat & Fluid Flow*, 28, 1930–1955.
- Izadi, M., Mohebbi, R., Karimi, D., & Sheremet, M. A. (2018). Numerical simulation of natural convection heat transfer inside a \perp shaped cavity filled by a MWCNT-Fe₃O₄/water hybrid nanofluids using LBM. *Chemical Engineering and Processing-Process Intensification*, 125, 56–66.
- Jaaz, A., Hasan, H., Sopian, K., Kadhum, A., Gaaz, T., & Al-Amieri, A. (2017). Outdoor performance analysis of a photovoltaic thermal (PVT) collector with jet impingement and compound parabolic concentrator (CPC). *Materials*, 10, 888.
- Jaaz, A. H., Sopian, K., & Gaaz, T. S. (2018). Study of the electrical and thermal performances of photovoltaic thermal collector-compound parabolic concentrated. *Results in Physics*, 9, 500–510.
- John, D., & Anderson, J. (1995). Computational fluid dynamics: the basics with applications. In *Mechanical Engineering Series*. Sydney: McGraw-Hill.
- Kherbeet, A. S., Mohammed, H., Salman, B., Ahmed, H. E., Alawi, O. A., & Rashidi, M. (2015). Experimental study of nanofluid flow and heat transfer over microscale backward- and forward-facing steps. *Experimental Thermal and Fluid Science*, 65, 13–21.
- Kumar, A., & Dhiman, A. K. (2012). Effect of a circular cylinder on separated forced convection at a backward-facing step. *International Journal of Thermal Sciences*, 52, 176–185.
- Kumar, S. S., Venkateswarlu, P., Rao, V. R., & Rao, G. N. (2013). Synthesis, characterization and optical properties of zinc oxide nanoparticles. *International Nano Letters*, 3, 30.
- Ma, Y., Mohebbi, R., Rashidi, M., & Yang, Z. (2018a). Study of nanofluid forced convection heat transfer in a bent channel by means of lattice Boltzmann method. *Physics of Fluids*, 30, 032001.
- Ma, Y., Mohebbi, R., Rashidi, M., & Yang, Z. (2019). MHD forced convection of MWCNT-Fe₃O₄/water hybrid nanofluid in a partially heated τ -shaped channel using LBM. *Journal of Thermal Analysis and Calorimetry*, 136(4), 1723–1735.
- Ma, Y., Mohebbi, R., Rashidi, M., & Yang, Z. (2018b). Simulation of nanofluid natural convection in a U-shaped cavity equipped by a heating obstacle: Effect of cavity's aspect ratio. *Journal of the Taiwan Institute of Chemical Engineers*, 93, 263–276.
- Ma, Y., Mohebbi, R., Rashidi, M., & Yang, Z. (2018c). Numerical simulation of flow over a square cylinder with upstream and downstream circular bar using lattice Boltzmann method. *International Journal of Modern Physics C*, 29, 1850030.
- Ma, Y., Mohebbi, R., Rashidi, M., Yang, Z., & Sheremet, M. A. (2019). Numerical study of MHD nanofluid natural convection in a baffled U-shaped enclosure. *International Journal of Heat and Mass Transfer*, 130, 123–134.
- Ma, Y., Mohebbi, R., Rashidi, M. M., Manca, O., & Yang, Z. (2018). Numerical investigation of MHD effects on nanofluid heat transfer in a baffled U-shaped

- enclosure using lattice Boltzmann method. *Journal of Thermal Analysis and Calorimetry*, 135(6), 3197–3213.
- Ma, Y., Mohebbi, R., Rashidi, M. M., & Yang, Z. (2019). Effect of hot obstacle position on natural convection heat transfer of MWCNTs-water nanofluid in U-shaped enclosure using lattice Boltzmann method. *International Journal of Numerical Methods for Heat & Fluid Flow*, 29, 223–250.
- Mohammed, H., Al-Aswadi, A., Shuaib, N., & Saidur, R. (2011). Convective heat transfer and fluid flow study over a step using nanofluids: a review. *Renewable and Sustainable Energy Reviews*, 15, 2921–2939.
- Mohammed, H., Al-Aswadi, A., Yusoff, M., & Saidur, R. (2012). Mixed convective flows over backward facing step in a vertical duct using various nanofluids-buoyancy-assisting case. *Thermophysics and Aeromechanics*, 42, 1–30.
- Mohammed, H., Alawi, O., & Sidik, N. C. (2016). Mixed convective nanofluids flow in a channel having forward-facing step with baffle. *Journal of Advanced Research in Applied Mechanics*, 24, 1–21.
- Mohammed, H., Alawi, O. A., & Wahid, M. (2015). Mixed convective nanofluid flow in a channel having backward-facing step with a baffle. *Powder Technology*, 275, 329–343.
- Mohebbi, R., & Heidari, H. (2017). Lattice Boltzmann simulation of fluid flow and heat transfer in a parallel-plate channel with transverse rectangular cavities. *International Journal of Modern Physics C*, 28, 1750042.
- Mohebbi, R., Izadi, M., & Chamkha, A. J. (2017). Heat source location and natural convection in a C-shaped enclosure saturated by a nanofluid. *Physics of Fluids*, 29, 122009.
- Mohebbi, R., Izadi, M., Delouei, A. A., & Sajjadi, H. (2019). Effect of MWCNT-Fe 3 O 4/water hybrid nanofluid on the thermal performance of ribbed channel with apart sections of heating and cooling. *Journal of Thermal Analysis and Calorimetry*, 135, 3029–3042.
- Mohebbi, R., Lakzayi, H., Sidik, N. A. C., & Japar, W. M. A. A. (2018). Lattice Boltzmann method based study of the heat transfer augmentation associated with Cu/water nanofluid in a channel with surface mounted blocks. *International Journal of Heat and Mass Transfer*, 117, 425–435.
- Mohebbi, R., Nazari, M., & Kayhani, M. (2016). Comparative study of forced convection of a power-law fluid in a channel with a built-in square cylinder. *Journal of Applied Mechanics and Technical Physics*, 57, 55–68.
- Mohebbi, R., & Rashidi, M. (2017). Numerical simulation of natural convection heat transfer of a nanofluid in an L-shaped enclosure with a heating obstacle. *Journal of the Taiwan Institute of Chemical Engineers*, 72, 70–84.
- Mohebbi, R., Rashidi, M., Izadi, M., Sidik, N. A. C., & Xian, H. W. (2018). Forced convection of nanofluids in an extended surfaces channel using lattice Boltzmann method. *International Journal of Heat and Mass Transfer*, 117, 1291–1303.
- Murshed, S. S., De Castro, C. N., Lourenço, M., Lopes, M., & Santos, F. (2011). A review of boiling and convective heat transfer with nanofluids. *Renewable and Sustainable Energy Reviews*, 15, 2342–2354.
- Nazari, M., Kayhani, M., & Mohebbi, R. (2013). Heat transfer enhancement in a channel partially filled with a porous block: lattice Boltzmann method. *International Journal of Modern Physics C*, 24, 1350060.
- Nazari, M., Mohebbi, R., & Kayhani, M. (2014). Power-law fluid flow and heat transfer in a channel with a built-in porous square cylinder: lattice Boltzmann simulation. *Journal of Non-Newtonian Fluid Mechanics*, 204, 38–49.
- Nie, J., & Armaly, B. F. (2002). Three-dimensional convective flow adjacent to backward-facing step-effects of step height. *International Journal of Heat and Mass Transfer*, 45, 2431–2438.
- Nikkhah, Z., Karimipour, A., Safaei, M. R., Forghani-Tehrani, P., Goodarzi, M., Dahari, M., et al. (2015). Forced convective heat transfer of water/functionalized multi-walled carbon nanotube nanofluids in a microchannel with oscillating heat flux and slip boundary condition. *International Communications in Heat and Mass Transfer*, 68, 69–77.
- Öztop, H. F. (2006). Turbulence forced convection heat transfer over double forward facing step flow. *International Communications in Heat and Mass Transfer*, 33, 508–517.
- Park, T. S., & Sung, H. J. (1995). A nonlinear low-Reynolds-number $k-\epsilon$ model for turbulent separated and reattaching flows—I. Flow field computations. *International Journal of Heat and Mass Transfer*, 38, 2657–2666.
- Patanker, S. (1980). *Numerical heat transfer and fluid flow*. New York: Hemisphere Publishing Corporation.
- Ranjbar, P., Mohebbi, R., & Heidari, H. (2018). Numerical investigation of nanofluids heat transfer in a channel consisting of rectangular cavities by lattice Boltzmann method. *International Journal of Modern Physics C (IJMPC)*, 29, 1–23.
- Rhee, G. H., & Sung, H. J. (1996). A nonlinear low-Reynolds-number $k-\epsilon$ model for turbulent separated and reattaching flows—II. Thermal field computations. *International Journal of Heat and Mass Transfer*, 39, 3465–3474.
- Richardson, H. W. (2002). *Copper compounds in Ullmann's encyclopedia of industrial chemistry*. Weinheim: Wiley-VCH.
- Safaei, M., Togun, H., Vafai, K., Kazi, S., & Badarudin, A. (2014). Investigation of heat transfer enhancement in a forward-facing contracting channel using FMWCNT nanofluids. *Numerical Heat Transfer, Part A: Applications*, 66, 1321–1340.
- Saidur, R., Leong, K., & Mohammad, H. (2011). A review on applications and challenges of nanofluids. *Renewable and Sustainable Energy Reviews*, 15, 1646–1668.
- Selimefendigil, F., & Öztop, H. F. (2015). Numerical investigation and reduced order model of mixed convection at a backward facing step with a rotating cylinder subjected to nanofluid. *Computers & Fluids*, 109, 27–37.
- Sheikholeslami, M., & Chamkha, A. J. (2016). Flow and convective heat transfer of a ferro-nanofluid in a double-sided lid-driven cavity with a wavy wall in the presence of a variable magnetic field. *Numerical Heat Transfer, Part A: Applications*, 69, 1186–1200.
- Sheikholeslami, M., & Ganji, D. (2016). Nanofluid convective heat transfer using semi analytical and numerical approaches: a review. *Journal of the Taiwan Institute of Chemical Engineers*, 65, 43–77.
- Trisakri, V., & Wongwises, S. (2007). Critical review of heat transfer characteristics of nanofluids. *Renewable and Sustainable Energy Reviews*, 11, 512–523.
- Tylli, N., Kaitkis, L., & Ineichen, B. (2002). Sidewall effects in flow over a backward-facing step: experiments and numerical simulations. *Physics of Fluids*, 14, 3835–3845.
- Vajjha, R. S., & Das, D. K. (2009). Experimental determination of thermal conductivity of three nanofluids and development of new correlations. *International Journal of Heat and Mass Transfer*, 52, 4675–4682.
- Wang, X.-Q., & Mujumdar, A. S. (2007). Heat transfer characteristics of nanofluids: a review. *International Journal of Thermal Sciences*, 46, 1–19.
- Williams, P., & Baker, A. (1997). Numerical simulations of laminar flow over a 3D backward-facing step. *International Journal for Numerical Methods in Fluids*, 24, 1159–1183.
- Xu, D., Pan, L., & Yao, Q. (2007). Heat transfer cost-effectiveness of nanofluids. In *Cleantech 2007: the Cleantech Conference, Venture Forum and Trade Show, May 23–24, 2007, Santa Clara, California, USA* (p. 79).
- Yu, W., & Xie, H. (2012). A review on nanofluids: preparation, stability mechanisms, and applications. *Journal of Nanomaterials*, 2012, 1.

Publisher's Note

Springer Nature remains neutral with regard to jurisdictional claims in published maps and institutional affiliations.

Submit your manuscript to a SpringerOpen[®] journal and benefit from:

- Convenient online submission
- Rigorous peer review
- Open access: articles freely available online
- High visibility within the field
- Retaining the copyright to your article

Submit your next manuscript at ► [springeropen.com](https://www.springeropen.com)